Journal of Sound and Vibration (1997) **205**(3), 257–264

EXPERIMENTAL DETERMINATION OF THE BUCKLING LOAD OF A STRAIGHT STRUCTURAL MEMBER BY USING DYNAMIC PARAMETERS

C. G. Go, Y. S. Lin and E. H. Khor

Department of Civil Engineering, National Chung Hsing University, Taichung, Taiwan, Republic of China

(*Received* 28 *October* 1994, *and in final form* 19 *July* 1995)

In engineering work, the handling of boundary conditions is not as perfect as required due to the present immaturity of engineering techniques. Hence the actual buckling load of an element is sometimes not consistent with that predicted in the design. For design considerations, the establishment of a method of analysis for determining the buckling load experimentally is necessary. The proposed approach is suitable for all kinds of boundaries, and an axial force is not required in the testing process. In practice, the dynamic parameters determined experimentally are utilized to calculate the buckling load.

1. INTRODUCTION

Buckling is a phenomenon in which a structural system can be given small displacements without application of a disturbing force [1]. Although this kind of phenomenon itself may not cause any damage in structural material, the consequence that hence a large displacement can result from a disturbing force may result in destruction of the structural system. Buckling is not merely caused by stress, but also by other factors such as the dimensions of the element, boundary conditions, material properties, etc. These factors may be controlled in engineering work, but nevertheless the handling of boundary condition is not as ideal as needed mostly because the actual buckling load deviated from that predicted in the design. Thus, it is necessary to establish an experimental method of determining the buckling load. Research efforts [2–8] in this field of study may be classified into two categories: the static approach and the dynamic approach. For the static approach, the implementation of a simulated load acting on the piece may not be easy in most cases. For the dynamic approach, the characteristic dynamic parameters related to the buckling load are the major considerations. Though several results have been obtained for particular cases, the analysis model still has to be improved for use in general cases. Herein, a method which is adaptable for all kinds of boundary conditions is proposed.

2. ANALYSIS MODEL

A structural member of length L with arbitrary end constraints is subjected to a compressive axial force, P, shown in Figure 1. For a small deformation, the x-axis configuration of the structural member is assumed to remain unchanged, but it experiences

0022–460X/97/330257 + 08 $25.00/0/sv951047

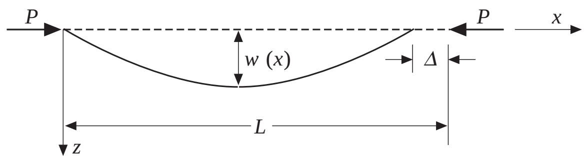

Figure 1. End displacement of a bent beam

a z-axis translation of $w(x)$. The total shortening distance Δ due to bending caused by the compressive axial load is [9]

$$D = \int_0^L \left[\sqrt{1 - \left(\frac{\mathrm{d}w(x)}{\mathrm{d}x} \right)^2} - 1 \right] \mathrm{d}x = \frac{1}{2} \int_0^L \left(\frac{\mathrm{d}w(x)}{\mathrm{d}x} \right)^2 \mathrm{d}x. \tag{1}$$

The work done by the applied compressive axial force P is

$$U = P \cdot D = \frac{P}{2} \int_0^L \left(\frac{\mathrm{d}w(x)}{\mathrm{d}x} \right)^2 \mathrm{d}x. \tag{2}$$

For convenience, the buckling shape of the structural member may be expressed by use of Lagrange's interpolation function $w(x)$ [10],

$$w(x) = \sum_{k=1}^{n} N_k(x) D_k, \tag{3}$$

where

$$N_k(x) = \frac{(x - x_1)(x - x_2) \cdots (x - x_{k-1})(x - x_{k+1})(x - x_{k+2}) \cdots (x - x_n)}{(x_k - x_1)(x_k - x_2) \cdots (x_k - x_{k-1})(x_k - x_{k+1})(x_k - x_{k+2}) \cdots (x_k - x_n)}. \tag{4}$$

D_k denotes the deflection at the interpolation point x_k. Substituting equation (3) into equation (2) yields

$$U = \frac{P}{2} \int_0^L \left(\sum_{k=1}^{n} \frac{\mathrm{d}N_k(x)}{\mathrm{d}x} D_k \right)^2 \mathrm{d}x. \tag{5}$$

The equivalent force F_i, corresponding to the deflection in the ith node may be obtained by using Castigliano's First Theorem [1] as

$$F_i = \partial U / \partial D_i = \sum_{k=1}^{n} \left[P \int_0^L \left(\frac{\mathrm{d}N_i}{\mathrm{d}x} \frac{\mathrm{d}N_k}{\mathrm{d}x} \right) \mathrm{d}x \right] D_k. \tag{6}$$

Equation (6) may be represented in matrix form as

$$\{\mathbf{F}\} = P[\mathbf{B}]\{\mathbf{D}\}, \tag{7}$$

where

$$[\mathbf{B}] = B_{ij} = \int_0^L \left(\frac{\mathrm{d}N_i}{\mathrm{d}x} \frac{\mathrm{d}N_j}{\mathrm{d}x} \right) \mathrm{d}x. \tag{8}$$

Also, the equivalent force F_i, may be related to the deflection D_i[1] by

$$\{\mathbf{D}\} = [\mathbf{G}]\{\mathbf{F}\}, \tag{9}$$

where [**G**] is called the flexibility matrix and its elements G_{ij} are called flexibility influence coefficients. G_{ij} is defined as the displacement at node j due to a unit load applied at node i.

Substituting equation (7) into equation (9) yields

$$\{\mathbf{D}\} = P[\mathbf{G}][\mathbf{B}]\{\mathbf{D}\}, \ \lambda\{\mathbf{D}\} = [\mathbf{G}][\mathbf{B}]\{\mathbf{D}\},$$

where $\lambda = 1/p$.

For a non-trivial solution one must have

$$|[\mathbf{G}][\mathbf{B}] - \lambda[\mathbf{I}]| = 0. \tag{10}$$

The solution for the maximum eigenvalue λ_{max}, is related to the buckling load P_{cr} by

$$P_{cr} = l/\lambda_{max}. \tag{11}$$

3. ESTABLISHMENT OF THE FLEXIBILITY MATRIX

The differential equation of free vibration for a structural member may be stated as

$$(\mathrm{d}^2/\mathrm{d}x^2)(EI\,\mathrm{d}^2w(x,t)/\mathrm{d}x^2) + m\,\mathrm{d}^2w(x,t)/\mathrm{d}t^2 = 0. \tag{12}$$

Assuming that the solution of equation (12) is separable into time and space factors, one may write

$$w(x,t) = \sum_{k=1}^{\infty} \phi_k(x)T_k(t). \tag{13}$$

Substituting equation (13) into equation (12) leads to two ordinary differential equations,

$$(\mathrm{d}^2/\mathrm{d}x^2)(EI\,\mathrm{d}^2\phi_k(x)/\mathrm{d}x^2) - m\omega_k^2\phi_k(x) = 0, \qquad \mathrm{d}^2T_k(t)/\mathrm{d}t^2 + \omega_k^2T_k(t) = 0, \quad (14, 15)$$

where ω_k and $\phi_k(x)$ are the natural frequency and the corresponding modal shape of the kth mode respectively.

The modal shape, $\phi_k(x)$ must satisfy the orthogonality condition

$$\int_0^L m\phi_i(x)\phi_j(x)\,\mathrm{d}x = \delta_{ij}, \tag{16}$$

where δ_{ij} is the Kronecker delta.

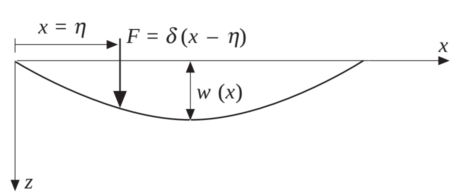

Figure 2. Dirac Delta function for loading and induced beam deflection

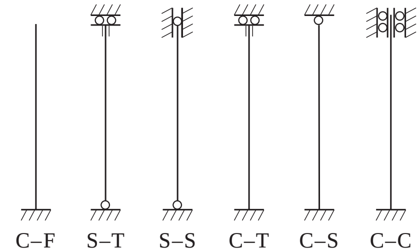

Figure 3. Prismatic beams for analysis on solution consideration

The equivalent equation of the above mentioned system which is subjected to a static unit load $F = \delta(x - \eta)$, at the position $x = \eta$ as shown in Figure 2, may be expressed as

$$(\mathrm{d}^2/\mathrm{d}x^2)(EI\mathrm{d}^2w(x)/\mathrm{d}x^2) = \delta(x - \eta). \tag{17}$$

By Galerkin's method, $w(x)$ may be approximated by a linear combination of function $(\phi_1, \phi_2, \phi_3, \cdots)$ as

$$w(x) = \sum_{k=1}^{\infty} a_k \phi_k(x), \tag{18}$$

where a_k are constants to be determined. Therefore,

$$\sum_{k=1}^{\infty} a_k \int_0^L \frac{\mathrm{d}^2}{\mathrm{d}x^2}\left(EI\frac{\mathrm{d}^2\phi_k(x)}{\mathrm{d}x^2}\right)\phi_i(x)\,\mathrm{d}x = \int_0^L \delta(x-\eta)\phi_i(x)\,\mathrm{d}x. \tag{19}$$

By comparing equation (14) with equation (17), the unknown constants a_k may be simplified by the use of equation (16) as

$$a_i = \phi_i(\eta)/\omega_i^2. \tag{20}$$

The deflection curve $w(x)$ may thus be obtained by substituting equation (20) into equation (18), to yield

$$w(x) = \sum_{k=1}^{\infty} \frac{\phi_k(\eta)\phi_k(x)}{\omega_k^2}. \tag{21}$$

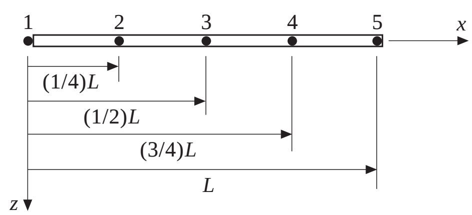

Figure 4. Uniform distributions of five stations for the analysis of buckling load.

TABLE 1

The buckling loads determined by means of uniform distribution of stations

End constraints	Exact solutions $P_{cr}(EI/L^2)$	Five stations $P_{cr}(EI/L^2)$	Five stations Errors (%)
C–F	2·4674	2·4694	0·08
S–T	2·4674	2·4595	−0·32
S–S	9·8696	9·8473	−0·22
C–T	9·8696	9·9640	−1·05
C–S	20·19	19·6541	−2·65
C–C	39·478	30·8129	−21·95

For $\eta = x_j$, the flexibility influence coefficient G_{ij} in equation (9) then be determined as

$$G_{ij} = w(x_i) = \sum_{k=1}^{\infty} \frac{\phi_k(x_i)\phi_k(x_j)}{\omega_k^2}. \tag{22}$$

4. SOLUTION CONSIDERATIONS

The interpolation function of equation (3) is used to describe the buckling shape, which plays a dominating role in the accuracy. With proper selection of interpolation points (i.e., stations in the experimentation) one may obtain a well-defined shape which leads to satisfactory solutions. Examples with extreme end constraints (i.e., free end and clamped end constraints) are chosen to illustrate the feasibility of the method.

4.1. EXAMPLE 1

The feasibility of the proposed approach is investigated by the analysis of prismatic beam with various end constraints, as shown in Figure 3, where S, C, F and T represent the simply supported, clamped, free and translation without rotation at the ends, respectively. Modal parameters used in constructing the simulated free-response functions were obtained from analytical solutions. The first five modes of vibration were considered. In this example, two different arrangements for distribution of the stations (i.e., equal and unequal distances between the stations) are considered. The exact solutions for the free vibration of the prismatic beam with various end conditions are also utilized to establish the flexibility matrix which is required for determining buckling load.

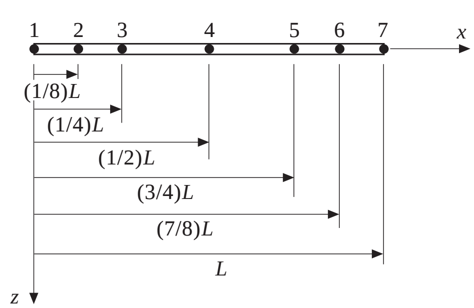

Figure 5. Non-uniform distributions of seven stations for the analysis of buckling load.

TABLE 2

The buckling load determined by means of non-uniform distribution of stations

End constraints	Exact solutions $P_{cr}(EI/L^2)$	Seven stations $P_{cr}(EI/L^2)$	Seven stations Errors (%)
C–F	2·4674	2·4599	−0·30
S–T	2·4674	2·4599	−0·30
S–S	9·8696	9·8434	−0·26
C–T	9·8696	9·8677	−0·01
C–S	20·19	20·0642	−0·62
C–C	39·478	39·2529	−0·57

4.1.1. *Uniform distribution of stations*

Five stations were selected to analyze the buckling load of the prismatic beam with various end conditions, as shown in Figure 4. The results are listed in Table 1. These results reveal that the prismatic beam with end conditions such as C–F, S–T, S–S and C–T are in very good agreement with the exact solutions, but not for cases C–S and C–C.

The main reason for this disagreement may be that the buckling shape function chosen does not represent properly the deflection of the structural member for the cases C–S and C–C. Actually, the buckling load is significantly affected by the effective length: that is, the distance between inflection points of the structure. For these two cases, inflection points do occur near the rigid end constraints. Therefore, in order to express the buckling deflection of the structural member thoroughly, one has to modify the distribution of the measuring stations. Herein, a non-uniform distribution of stations approach is proposed to improve the precision of the identified results.

4.1.2. *Non-uniform distribution of stations*

For the non-uniform distribution of stations method, only seven stations were selected for analyzing the buckling load, in which five of the stations were located at the same positions as before, and the remaining two stations were placed in the interval between the points ($x = 1/4\,L$, $3/4\,L$) and the end points ($x = 0, L$), as shown in Figure 5. The identified results are listed in Table 2. The identified results are sufficiently good in comparison with the exact solution for all cases.

4.2. EXAMPLE 2

The second example is for end conditions of line spring and rotation spring support, as shown in Figure 6. The flexibility matrix of this example is determined by dynamic parameters derived from a finite element method. The spring constants are $\alpha_1 = 15\,EI/L^3$, $\alpha_2 = 50\,EI/L^3$ and $\beta = 100\,EI/L^2$, respectively. In this example, five equi-distance measuring stations and seven non-equi-distant measuring stations were chosen for

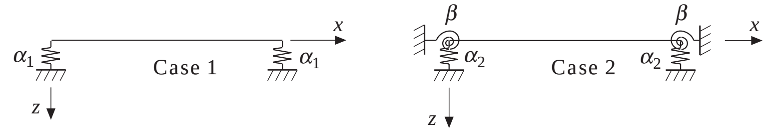

Figure 6. Beam with spring supports as example for buckling load determination.

TABLE 3

Results for spring end constraints compared with these derived from the finite element method

End constraints	Finite element $P_{cr}(EI/L^2)$	Uniform distribution of stations (5 stations) $P_{cr}(EI/L^2)$	Uniform distribution of stations (5 stations) Errors (%)	Non-uniform distribution of stations (7 stations) $P_{cr}(EI/L^2)$	Non-uniform distribution of stations (7 stations) Errors (%)
Case 1	7·500	7·492	−0·11	7·492	−0·11
Case 2	29·228	27·590	−5·60	28·623	−2·06

determining the buckling load. The results, together with those from the finite element method, are listed in Table 3. From this table, it is not difficult to discover that the analysis model in which seven non-equi-distant measuring points was used determine the buckling load relatively correctly for arbitrary end constraints.

These two examples indicate that the distribution of the measuring points on the structural member plays a significant role in determining the buckling load. Using seven non-equi-distant measuring stations is a commendable means for determination of the buckling load.

5. FEASIBILITY OF EXPERIMENTAL IDENTIFICATION

In practice, the accuracy of the experimental determination of the buckling load is always affected by factors such as experimental apparatus error, man-made error, etc. To assess the possible error for the buckling load determination, a simulation experimentation was designed and carried out, as follows: (1) calculation of theoretical vibration parameters $[\bar{\phi}]$ and $\bar{\omega}_n$; (2) generation of experimental errors e within an error range by using the Monte-Carlo method [12]; (3) simulation of experimental vibration parameters $[\phi]$ and ω_n by the formulas $\phi_i = \bar{\phi}_i \times (1 + e_i)$ and $\omega_n = \bar{\omega}_n \times (1 + e_n)$; (4) determination of $[\mathbf{G}]$ by using equation (22); (5) determination of $[\mathbf{B}]$ by using equation (8); (6) identification of P_{cr} by using equation (11).

In the analysis, three different cases, with error ranges, 2%, 4% and 6% were taken into consideration. With 10 000 simulation experimentations in each case, the maximum error of P_{cr} for different boundary conditions are shown in Table 4. It may be inferred that the accuracy of the buckling load identification is proportional to the measurement errors. Since the technique of model testing is well-established, an identification error within 3% can easily be reached. This means, from Table 4, that the proposed approach can provide an effective way to determine the buckling load.

TABLE 4

Maximum % errors of simulation experimentations for various end conditions

Experimental error range (%)	S–S	C–F	S–C	C–C
2	5	8	5	8
4	10	14	10	14
6	15	20	15	20

6. CONCLUSION

An analysis model for determining the buckling load of a structural member by utilizing dynamic parameters determined experimentally is proposed in this paper. It is concluded that the proposed analysis model is a valid method for determining the buckling load. The main advantages of applying the proposed analysis model may be stated as follows: (1) it requires only the dynamic parameters, i.e., natural frequencies and the corresponding mode shapes, for buckling load determination, (2) it is suitable for all kinds of end constraints: (3) there is no axial force required in the process.

REFERENCES

1. A. Ghali and A. N. Neville 1978 *Structural Analysis*. London: Chapman and Hall Ltd.
2. R. Lurie 1952 *Journal of Applied Mechanics* **19**, 195–203. Lateral vibration as related to structural stability.
3. A. L. Sweet and J. Genin 1971 *Journal of Sound and Vibration* **14**, 317–324. Identification of a model for predicting elastic buckling.
4. M. Baruch 1973 *Israel Journal of Technology* **11**, 1–8. Integral equations for nondestructive determination of buckling loads for elastic plates and bars.
5. A. L. Sweet, J. Genin and P. F. Mlakar 1976 *Journal of Dynamic Systems*, *Measurement and Control*, **98,** 387–394. Vibratory identification of beam boundary conditions.
6. A. L. Sweet, J. Genin and P. F. Mlakar 1977 *Experimental Mechanics* **17**, 385–391. Determination of column buckling criteria using vibratory data.
7. A. Segall and M. Baruch 1980 *Experimental Mechanics* **20**, 285–288. A nondestructive dynamic method for determination of the critical load of elastic column.
8. A. Segall and G. S. Springer 1986 *Experimental Mechanics* **26**, 354–359. A dynamic method for measuring the critical loads of an elastic flat plate.
9. S. P. Timoshenko and J. M. Gere 1984 *Theory of Elastic Stability*. New York.
10. O. C. Zienkiewicz and R. L. Taylor 1989 *The Finite Element Method*, *Volume* 1, *Basic Formulation and Linear Problem*. New York: McGraw Hill. See p. 119.
11. R. L. Bisplinghoff, H. Ashley and R. L. Halfman 1955 *Aeroelasticity*. New York: Addison–Wesley. see pp. 68–95.
12. F. S. Hiller and Q. J. Liberman 1974 *Operations Research*. San Francisco: Hoden-Day. see pp. 621–649.